Synthesis and Characterization of Novel Heteroleptic Ruthenium Complexes for Dye-Sensitized Solar Cells

Wei-Kai Huang[a] (黃威凱), Chi-Ming Lan[a] (藍啓銘), Yu-Sin Liu[b] (劉育欣), Pei-Heng Lee[b] (李佩恆), Shu-Mei Chang[b,*] (張淑美) and Eric Wei-Guang Diau[a,*] (刁維光)

[a]*Department of Applied Chemistry and Institute of Molecular Science, National Chiao Tung University, Hsinchu, Taiwan 30010, R.O.C.*

[b]*Institute of Organic and Polymeric Materials, National Taipei University of Technology, Taipei 106, Taiwan, R.O.C.*

We report three novel heteroleptic ruthenium complexes, RD1: Ru[(dcbpy)(1-methyl-2-(pyridin-2-yl)-1H-benzimidazole)$(NCS)_2$, RD2: Ru [(dcbpy) (2-(pyridine-2-yl) benzothiazole) $(NCS)_2$, and RD3: Ru[(dcbpy)(2-(pyridin-2-yl) benzoxazole) $(NCS)_2$, for dye-sensitized solar cell applications. We found that RD1 exhibits a dye loading amount two times higher than that of N719, which gives a broad IPCE action spectrum for the spectral response beyond 800 nm. This series of dyes can be easily synthesized in three steps with the best dye (RD1) reaching 80 % cell performance of N719.

Keywords: DSSC; Heteroleptic; Imidazole; Ruthenium complexes; Solar cells.

INTRODUCTION

Dye-sensitized solar cells (DSSC) based on mesoporous nanocrystalline TiO_2 films have attracted much attention for scientific and industrial applications owing to their high photon-to-electricity conversion efficiency and low production cost.[1] Ruthenium complexes, such as N3, N719 and black dyes, have been extensively utilized as photosensitizers, and high power conversion efficiencies over 10 % were reported in the devices based on these dyes.[2] Moreover, the color tunable, high absorption coefficient metal-free organic dyes,[3] non-ruthenium metal center dyes,[4] and porphyrin-based green sensitizers[5] have been widely discussed and reported in recent years. In addition to the polypyridine-based ruthenium complexes being widely investigated, the heterocyclic ligands have also been applied to make ruthenium complexes.[6] In the present study, we have designed new ruthenium dyes by replacing one of the 2,2′-bipyridine-4,4′-dicarboxylic acid (dcbpy) ligands of N3 with three easily synthesized heterocylic ligands, namely oxazole, thiazole, and imidazole derivatives, for which they were used to make corresponding ruthenium complexes for DSSC applications.

EXPERIMENTS

Materials

All reagents and solvents were obtained from commercial sources and used without further purification unless otherwise noted. DMF used for electrochemistry was dried over $MgSO_4$ and freshly distilled before use. CH_3CN was dried over CaH_2 and freshly distilled before use. Tetra-*n*-butylammonium hexafluorophosphate ($TBAPF_6$) was recrystallized twice from absolute ethanol and further dried for two days under vacuum. Column chromatography was performed on silica gel (70-230 Mesh ASTM, Merck). Sephadex LH-20 column was obtained from GE.

Instrumentation

Absorption spectra were recorded on UV-vis spectrometer (Varian, Cary 50). NMR data were obtained on a Bruker DRX-300 Spectrometer. The measurements of PL spectra were performed by using a Spex Fluorolog-3 spectrofluorometer (Instruments S.A., Edison, N.J., USA). Elemental analyses were carried out on an Elemental analyzer (Foss Heraeus, CHN-O-RAPID). Mass Spectroscopy measurements were performed on a Mass Spectrometer (MICRO- MASS, TRIO-2000). For certain cyclic voltammetry experiments were measured by a potentiometer (potentiosatate/Galvan model 273, EG&G).

Synthesis of ligands

1-methyl-2-(pyridin-2-yl)benzimidazole (L1)[7]

Under nitrogen atmosphere, picolinic acid (2.46 g, 0.02 mol), N-methylbenzene- 1,2-diamine (2.44 g, 0.02 mol), and polyphosphoric acid (PPA, 10 g) were heated to

Special Issue for the 2009 International Symposium of Dye-Sensitized Solar Cells

* Corresponding author. Tel: +886-3-5131524; Fax : +886-3-5723764; E-mail: diau@mail.nctu.edu.tw

150 °C for 2 h. After cooling, the solution was poured into cool water with stirring, and tune the pH to 7-8 by addition of NaOH, and the resulting gray/pink precipitate was filtered, wash with water, and air dried. The crude product was purified by column chromatography (silica gel) using a mixture of ethyl acetate and hexane (1/3) as an eluent (2.15 g, 55 %).

2-(pyridin-2-yl)benzothiazole (L2)[8]

Under nitrogen atmosphere, picolinic acid (2.46 g, 0.02 mol), 2-aminothiophenol (2.5 g, 0.02 mol), and PPA (10g) were heated to 150 °C for 2 h. After cooling, the solution was poured into cool water with stirring. The resulting gray/white precipitate was collected by filtration, washed with water and dried, re-crystallized from ethanol (2.63 g, 62 %).

2-(pyridin-2-yl)benzoxazole (L3)[9]

Under nitrogen atmosphere, picolinic acid (2.46 g, 0.02 mol), 1,2-benzenediol (2.2 g, 0.02 mol), and PPA (10g) were heated to 150 °C for 2 h. After cooling, the solution was poured into cool water with stirring, and tune the pH to 7-8 by addition of NaOH, and the resulting gray/pink precipitate was filtered, wash with water, and air dried. The crude product was purified by column chromatography (silica gel) using a mixture of ethyl acetate and hexane (1/1) as an eluent (2.33 g, 59.4 %).

Synthesis of complexes

[Ru(4,4′-carboxylicacid-2,2′-bipyridine) (1-methyl-2-(pyridine-2-yl)-1H-benzoimidazole)NCS_2] – RD1

In a typical one-pot synthesis,[10] $[RuCl_2(p\text{-}cymene)]_2$ (108 mg, 0.176 mmol) was dissolved in DMF (20 mL) and the precursor ligand L1 (73.6 mg, 0.352 mmol) was added. The reaction mixture was heated at 80 °C under argon for 4 h and then dcbpy (86 mg, 0.352 mmol) was added. The reaction mixture was refluxed at 140 °C for another 4 h in dark to avoid the photoinduced cis-to-trans isomerization. Excess KNCS was added to the reaction mixture and heated at 140 °C for 5 h. After the reaction, the solvent was removed by using a rotary evaporator. Water was added to the resulting mixture to remove any excess KNCS. The water-insoluble product was then collected on a sintered-glass crucible by suction filtration, washed with distilled water, followed by diethyl ether, and dried in air. The crude product was dissolved in methanol then passed through Sephadex LH-20 column using methanol as the eluent. The main band was collected and concentrated. The same purification was repeated for five times. A few drops of 0.01M HNO_3 (aq) were added to precipitate the brown red product (71 mg, 33.9 %).

[Ru(4,4′-carboxylic acid-2,2′-bipyridine)(2-(pyridine-2-yl)benzothiazole) NCS_2] – RD2

Same procedure as preparing RD1 but the ligand L2 (75mg, 0.352 mmol) instead of L1 was used, resulting in dark purple powder (61 mg, 25.8 %).

[Ru(4,4′-carboxylic acid-2,2′-bipyridine)(2-(pyridine-2-yl) benzoxazole) NCS_2] –RD3

Same procedure as preparing RD-1 but the ligand L3 (69 mg, 0.352 mmol) instead of L1 was used, resulting in red purple powder (55 mg, 23.7 %).

Product characterizations

Ligands

L1: ^{1}H-NMR(DMSO-d_6) δ 8.76 (d, *J* = 4.0 Hz, 1H), 8.31 (d, *J* = 7.6 Hz, 1H), 8.01 (ddd, *J* = 8.0, 8.0, 1.6 Hz, 1H), 7.73 (d, *J* = 8.0 Hz, 1H),7.65 (d, *J* = 8.0 Hz, 1H), 7.53 (ddd, *J* = 7.6, 4.8, 0.8 Hz, 1H), 7.34 (ddd, *J* = 7.6, 7.2, 1.6 Hz, 1H) 7.28(ddd, *J* = 7.5, 6.8, 0.8 Hz, 1H) 4.24(s, 3H), Mass, EI-mass: calcd *m/z*: 209.10; Found: 208.

L2: ^{1}H-NMR(DMSO-d_6) δ 8.70 (d, *J* = 4.4 Hz, 1H), 8.30 (d, *J* = 8.4 Hz, 1H), 8.14 (d, *J* =7.2 Hz, 1H), 8.08 (d, *J* = 8.0 Hz, 1H), 8.05 (ddd, *J* = 8.0, 8.0, 2.0 Hz, 1H), 7.63-7.56 (m, 2H), 7.51 (ddd, *J* = 7.6, 7.2, 1.2 Hz, 1H), Mass, EI-mass: calcd *m/z*: 212.04; Found: 212.

L3: ^{1}H-NMR (DMSO-d_6) δ 8.81 (d, *J* = 4.8 Hz, 1H), 8.36 (d, *J* = 8.0 Hz, 1H), 8.08 (ddd, *J* = 9.0, 6.8, 1.6 Hz, 1H), 7.89 (d, *J* = 7.2 Hz, 1H), 7.86 (d, *J* = 8.0 Hz, 1H) 7.65 (dd, *J* = 7.2, 4.8 Hz, 1H), 7.53-7.45 (m, 2H), Mass, EI-mass: calcd *m/z*: 196.06; Found: 196.

Complexes

RD1: Elemental analysis (%) calcd for $C_{27}H_{19}N_7O_4S_2Ru\cdot H_2O\cdot 2CH_3OH$: C 46.27, H 3.88, N 13.02; Found: C 46.10, H 3.87, N 12.78. Mass, LRMS (FAB): calcd *m/z:* 671.0; Found: 671.0 (m).

RD2: Elemental analysis (%) calcd for $C_{26}H_{16}N_6O_4S_3Ru\cdot H_2O\cdot 2CH_3OH$: C 43.73, H 3.41, N 10.96; Found: C 43.72, H 3.26, N 11.33. Mass, LRMS (FAB): calcd *m/z*: 673.94; Found: 674.0 (m).

RD3: Elemental analysis (%) calcd for $C_{26}H_{16}N_6O_5S_2Ru\cdot H_2O\cdot 2CH_3OH$: C 45.46, H 3.54, N 11.36; Found: C 45.30, H 3.51, N 11.60. Mass, LRMS (FAB): calcd *m/z*: 657.97; Found: 658.0 (m).

Electrode preparation and device fabrication

The photoanodes composed of nanocrystalline TiO_2 were prepared using the sol-gel method reported elsewhere.[11] A paste composed of ~15-nm TiO_2 particles for the transparent nanocrystalline layer was coated on a

$TiCl_4$-treated FTO glass substrate (FTO, 8 Ω/ϒ) by repetitive screen printing to obtain the required film thickness. To improve the performance of DSSC, one additional scattering layer (particle size 200-600 nm) was screen-printed on the transparent nanocrystalline layer. The TiO_2 working electrodes were gradually heated according to a programmed procedure: (1) heating at 80 °C for 15 min; (2) heating at 135 °C for 10 min; (3) heating at 325 °C for 30 min; (4) heating at 375 °C for 5 min; (5) heating at 450 °C for 15 min; (6) heating at 500 °C for 15 min. The resulting layer was composed of 12-μm thickness of transparent layer and 4-μm thickness of scattering layer, which were treated again by $TiCl_4$ at 70 °C for 30 min and sintered at 500 °C for 30 min. After cooling in air, the sintered TiO_2 films were immersed in dye solutions (0.3 mM in anhydrous CH_3CN/t-BuOH (1:1 v/v) at 25 °C for 3 h) containing CDCA 0.3 mM for dye loading onto the working electrodes. The counter electrode was made by spin-coating the H_2PtCl_6/isopropanol solution onto an FTO glass substrate (FTO, 8 Ω/ϒ) (typical size 1.0 × 1.5 cm^2) through thermal decomposition at 380 °C for 30 min. The two electrodes were assembled into a cell of sandwich type and sealed with a hot-melt film (SX1170, thickness 25 μm). The electrolyte solution for devices contains 1.0 M 1-butyl-3-methyl- imidazolium iodide (BMII), 0.1 M guanidinium thiocyanate, 0.05 M LiI, 0.03 M I_2, and 0.5 M 4-tertbutylpyridine(TBP) in a solvent mixture containing acetonitrile and valeronitrile (volume ratio 85:15).[12]

Dye-loading examination

To determine the dye-loading amount of RD1-RD3 and N719 on TiO_2 films, the dye was desorbed in tetrabutylammonium hydroxide (0.1 M, TBAOH, Fluka) in DMF (3 mL). The absorption spectrum of the solution was recorded with a UV-vis spectrometer. A calibration curve for dyes in 0.1 M TBAOH in DMF was derived to obtain the absorption coefficient. The amounts of dye coverage on TiO_2 films were obtained from the measured absorbances in the spectra (cuvette thickness 2 mm) and the calibrated absorption coefficient of dyes according to Beers' law.

Photovoltaic characterization

The current-voltage characteristics were determined with a digital source meter (Keithley 2400, computer-controlled) with the device under one-sun AM 1.5 irradiation from a solar simulator (SAN-EI, XES-502S) calibrated with a standard silicon reference cell (VLSI standards, Oriel PN 91150V). When the device is irradiated with the solar simulator, the source meter sends a voltage (V) to the device, and the photocurrent (I) is read at each step controlled with a computer via a GPIB interface. The efficiency (η) of conversion of light to electricity is obtained with these relations, $\eta = J_{SC}\, V_{OC}\, FF / P_{in}$, in which J_{SC} /mA cm^{-2} is the current density measured at short circuit, and V_{OC} /V is the voltage measured at open circuit. P_{in} is the input radiation power (for one-sun illumination P_{in} = 100 mW cm^{-2}) and FF is the fill factor. For all measurements, the DSSC devices were covered with a black mask of aper-

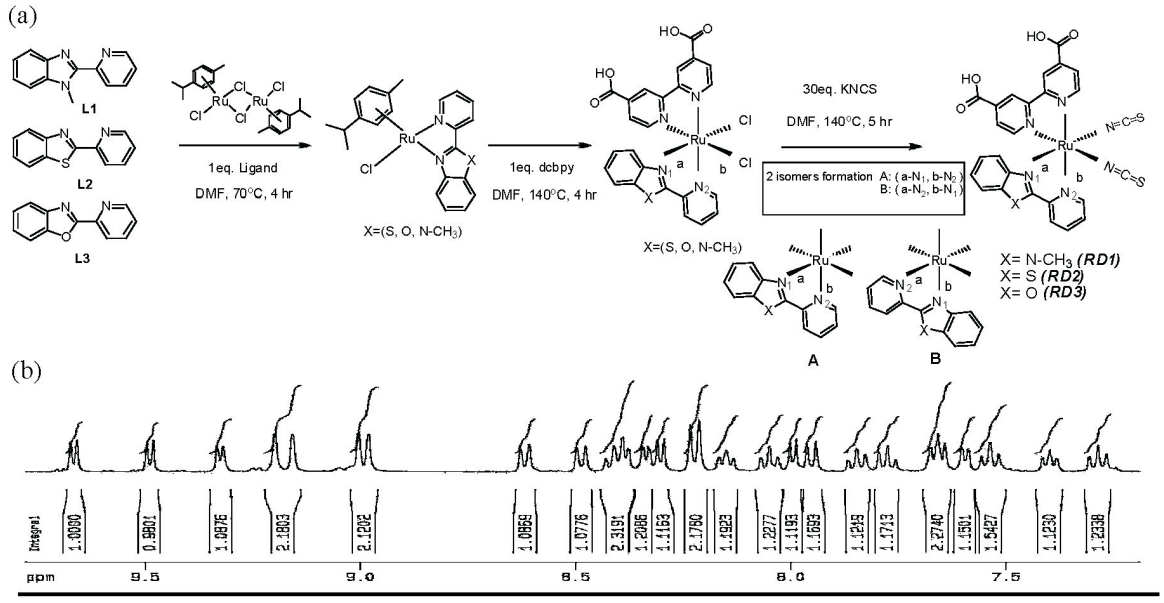

Fig. 1. (a) The synthesis flow chart for RD1-RD3; (b) ^{1}HNMR spectrum (7~10 ppm) of RD3.

Table 1. Absorption coefficients (ε/cm^{-1}M^{-1}), absorption maxima (λ_{max}/nm, in parenthesis) and electrochemical data of RD1-RD3, and N719

Dyes[a]	$\varepsilon_{\pi-\pi^*}(\lambda_{max})$	$\varepsilon_{\pi-\pi^*}$ or ε_{MLCT} (λ_{max})	ε_{MLCT} (λ_{max})	E_{ox} /V[b]	E_{0-0} /V[c]	E_{LUMO} /V[d]
N719	49154 (310 nm)	13400 (384 nm)	13610 (524 nm)	–	–	–
RD1	30704 (317nm)	6324 (403nm)	7560 (539nm)	0.93	1.92	-0.99
RD2	26168 (315nm)	5354 (381nm)	6850 (549nm)	0.98	1.85	-0.87
RD3	30686 (314nm)	5795(382nm)	7383 (537nm)	1.00	1.86	-0.86

[a] Absorption spectra were measured in DMF.

[b] Oxidation potential E_{OX} (V vs F/Fc$^+$) of dyes were measured in dry DMF with 0.1M (η-C_4H_9)$_4$NPF$_6$ with a scan rate of 50 mV s^{-1} (vs NHE).

[c] E_{0-0} was determined from the intersection of absorption and emission spectra in DMF.

[d] E_{LUMO} was calculated by $E_{OX} - E_{0-0}$.

Table 2. Photovoltaic parameters of RD1-RD3 and N719 sensitized solar cells under AM1.5 illumination (power 100 mW cm^{-2}) with an active area of 0.16 cm^2 with a black mask

Dyes	J_{SC} /Ma cm^{-2}	V_{OC} /V	*FF*	η (%)	Dye Loading/nmol cm^{-2}
N719	14.157	0.783	0.69	7.69	154
RD1	13.137	0.701	0.68	6.22	300
RD2	10.107	0.731	0.70	5.19	275
RD3	9.105	0.741	0.70	4.71	236

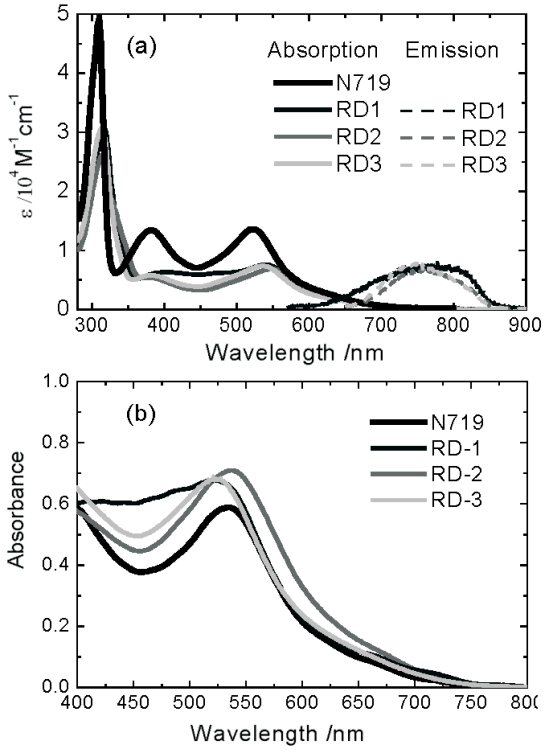

Fig. 2. Absorption spectra of (a) RD1-RD3 and N719 in DMF (2×10^{-5}M) and (b) RD1-RD3 and N719 absorbed onto 2-μm TiO_2 films.

ture area 0.16 cm^2 to ensure the measured photocurrent not being exaggerated. The spectra of the incident photons-to-current conversion efficiency (IPCE) of the corresponding devices were obtained with a system comprising a Xe lamp (PTi A-1010, 150 W), a monochromator (Dongwoo DM150i, 1200 gr/mm blazed at 500 nm), and a source meter (Keithley 2400).[13]

RESULTS AND DISCUSSION

Synthesis

As indicated in Fig. 1a, we synthesized three novel ruthenium complexes, RD1, RD2, and RD3, with heterocyclic ligands of imidazole, thiazole, and oxazole derivatives, respectively. We found that the final complexes with unsymmetric ligands have two isomers (A and B, see Fig. 1a) and they cannot be separated by using the silica, aluminum oxide, and Sephadex LH-20 column chromatography methods. Fig. 1b displays the ^{1}H-NMR spectrum of RD3 showing the groups of doublet/multiple peaks in the 7-10 ppm region. The integration of the peak areas indicates that the isomer ratio of A/B is 1:1.

Absorption Spectra and dye-loading

Fig. 2a shows the UV-Visible absorption spectra of RD1, RD2, and RD3 in DMF, compared with that of N719. We found that the molar absorption coefficients of the lower energy MLCT bands of RD1 (ε /M^{-1}cm^{-1} = 7560), RD2 (ε /M^{-1}cm^{-1} = 6850) and RD3 (ε /M^{-1}cm^{-1} = 7383) are significantly lower than that of N719 (ε /M^{-1}cm^{-1} = 13610), but the absorbances of RD1-RD3 absorbed on TiO_2 films are much higher than those of N719 (Fig. 2b). As a result, the amounts of dye loading of RD1-RD3 are in general two times higher than that of N719 (Table 2). Even though the

molar absorption coefficient of RD1 was not so great, the substantial dye loading enhancement of RD1 (300 nmol cm^{-2}) led to a high photocurrent density (13.137 mA cm^{-2}).

Electrochemistry

To evaluate the possibility of electron transfer from the excited state of the dye to the conduction band of TiO_2 electrode, we have performed cyclic voltammetry measurements for RD1, RD2, and RD3 in DMF with $TBAPF_6$. The oxidation potentials (E_{ox}) of RD1, RD2, and RD3 were measured to be 0.93, 0.98, and 1.00V versus NHE, respectively. The uphill energy offset of the HOMO in those dyes relative to that (+0.5 V) of the triiodide/iodide couple could lead to fast dye regeneration. The LUMO potentials (E_{LUMO}) of RD1, RD2, and RD3 calculated from the oxidation potentials and the band gaps (E_{0-0}) determined from the intersection of absorption and emission spectra[14] are -0.99V, -0.87V, and -0.86V, respectively (Table 1). The downhill energy offset of the LUMO in all dyes compared to the conduction band level of TiO_2 ensures enough driving force for charge separation.

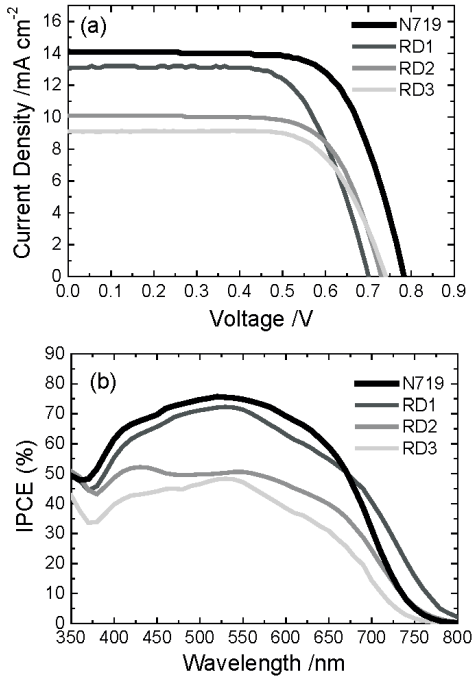

Fig. 3. (a) *I-V* characteristics of RD1-RD3 and N719 sensitized solar cells under AM 1.5 one-sun irradiation (100 mW cm^{-2}) and an active area of 0.16 cm^2 with a black mask; (b) The corresponding IPCE action spectra of RD-1-RD3 and N719.

Photovoltaic Measurements

In comparison with N719, the current-voltage characteristics of RD1-RD3 under 1.5G illumination (100 mW cm^{-2}) are shown in Fig. 3a and the corresponding photovoltaic parameters are listed in Table 2. The open-circuit photovoltage of RD1-RD3 are V_{OC} /V = 0.701, 0.731, and 0.741 respectively, showing the effect of different substitute of the five-member ring (N-CH_3, S, or O) of the ligand. This might be explained by their oxidation potentials, which show the increasing order for RD1 (0.93 V) > RD2 (0.98 V) > RD3 (1.00 V). The incident photon-to-current conversion efficiencies (IPCE) of RD1-RD3 are presented in Fig. 3b. The IPCE spectrum of RD1 exhibits a red shift spectral feature beyond 800 nm, which might be due to the enhanced dye loading of RD1 that boosts up the photocurrent response in the Near-IR region for higher photocurrent density (J_{SC} = 13.137 mA cm-2) being observed. On the other hand, both RD2 and RD3 show much lower J_{SC} values due to their much lower IPCE values. We expect that the imidazole ligand with stronger electron donating property might lead to better charge separation so that the charge-collection efficiency of RD1 becomes much larger than those of RD2 and RD3. Further time-resolved investigations are underway to understand the electron lifetimes and charge-transport kinetics of the system.

CONCLUSION

In summary, we have synthesized three novel heteroleptic ruthenium dyes (RD1, RD2, and RD3) for DSSC applications. Compared with the dcbpy ligand used in N3 dye, these unsymmetrical ligands were easy to synthesize with larger dye loading on TiO_2 surface than that of N719. RD1 reaches 80 % cell performance of N719, and it is the best among these three dyes due to its larger dye loading and broader IPCE action spectrum. However, the molar absorption coefficients of this series of dyes are much lower than that of N719. Therefore, future work aiming at the design of new series of heteroleptic Ru dyes with higher molar absorption coefficient is underway.

ACKNOWLEDGEMENT

National Science Council of Taiwan and Ministry of Education of Taiwan, under the ATU program, provided support for this project.

Received December 8, 2009.

REFERENCES

1. (a) O'Regan, B.; Grätzel, M. *Nature* **1991**, *353*, 737 (b) Nazeeruddin, M. K.; Kay, A.; Rodicio, I.; Humphry-Baker, R.; Muller, E.; Liska, P.; Vlachopoulos, N.; Grätzel, M. *J. Am. Chem. Soc.* **1993**, *115*, 6382 (c) Grätzel, M. *Inorg. Chem*. **2005**, *44*, 6841.
2. (a) Grätzel, M. *Nature* **2001**, *414*, 338 (b) Kurger, J.; Plass, R.; Bach, U.; Humphry-Baker, R.; Horiuchi, T.; Miura, H.; Ito, S.; Uchida, S.; Grätzel, M. *Adv. Mater.* **2005**, *17*, 813. (c) Schmidt-Mende, L.; Zakeeruddin, S. M.; Grätzel, M. *Appl. Phys. Lett.* **2005**, *86*, 13504 (d) O'Regan, B.; Lenzmann, F.; Muis, R.; Wienke, J. *Chem. Mater.* **2002**, *14*, 5023.
3. (a) Zhang, G.; Bala, H.; Cheng, Y.; Shi, D.; Lv, X.; Yu, Q.; Wang, P. *Chem. Commun.* **2009**, 2198. (b) Ito, S.; Miura, H.; Uchida, S.; Takata, M.; Sumioka, K.; Liska, P.; Comte, P.; Pechy, P. Grätzel, M. *Commun.* **2008**, 5194. (c) Kim, S.; Lee, J. K.; Kang, S. O.; Ko, J.; Yum, J.-H.; Fantacci, S.; de Angelis, F.; di Censo, D.; Nazeeruddin, M. K.; Grtäzel, M. *J. Am. Chem. Soc.* **2006**, *128*, 16701.
4. Kumaresan, D.; Thummel, R. P.; Bura T.; Ulrich, G.; Ziessel, R. *Chem. Eur. J.* **2009**, *15*, 6335.
5. (a) Lee, C.-W.; Lu, H.-P.; Lan, C.-M.; Huang, Y.-L.; Liang, Y.-R.; Yen, W.-N.; Liu, Y.-C.; Lin, Y.-S.; Diau, E. W.-G.; Yeh, C.-Y. *Chem. Eur. J.* **2009**, *15*, 1403. (b) Lu, H.-P.; Mai, C.-L.; Tsia, C.-Y.; Hsu, S.-J.; Hsieh, C.-P.; Chiu, C.-L.; Yeh, C.-Y.; Diau, E. W.-G. *Phys. Chem. Chem. Phys.* **2009**, *11*, 10270. (c) Hsieh, C.-P.; Lu, H.-P.; Chien, C.-L.; Lee, C.-W.; Chuang, S.-H.; Mai, C.-L.; Yen, W.-N.; Hsu, S.-J.; Diau, E. W.-G.; Yeh, C.-Y. *J. Mater. Chem.* **2010**, *20*, 1127. (d)Lu, H.-P.; Tsai, C.-Y.; Yen, W.-N.; Hsieh, C.-P.; Lee, C.-W.; Yeh, C.-Y.; Diau, E. W.-G. *J. Phys. Chem. C* **2009**, *113*, 20990. (e) Mai, C.-L.; Huang, W.-K.; Lu, H.-P.; Lee, C,-W.; Chiu, C.-L.; Liang, Y.-R.; Diau, E. W.-G.; Yeh, C.-Y. *Chem. Commun.* **2010**, *46*, 809.
6. (a) Wang, P.; Humphry-Baker, R.; Moser, J. E.; Zakeeruddin, S. M.; Grätzel, M. *Chem. Mater.* **2004,** *16,* 3246. (b) Jin, Z.; Mazuda, H.; Yamanaka, N.; Minami, M.; Nakamura, T.; Nishikitani, Y. *J. Phys. Chem. C*. **2009**, *113*, 2618. (c) Kim, J. J.; Choi, H.; Kim, C.; Kang, M.-S.; Kang, H. S.; Ko, J. *Chem. Mater.* **2009**, *21*, 5719.
7. Addison, A. W.; Rao, N. T.; Wahlgren, C. G. *J. Heterocycl. Chem.* **1983**, *20*, 1481.
8. Czerwieniec, F.; Kapturkiewicz, A.; Lipkowski, J.; Nowacki, J. *Inorg. Chim. Acta* **2005**, *358*, 2701.
9. Haugwitz, R. D.; Angel, R. G.; Jacobs, G. A. *J. Med. Chem.* **1982**, *25*, 969.
10. Klein, C.; Nazeeruddin, M. K.; Liska, P.; Dicenso, D.; Hirata, N.; Palomares, E.; Durrant, J. R.; Grätzel, M. *Inorg. Chem*. **2005**, *44*, 178.
11. (a) Ito, S.; Chen, P.; Comte, P.; Nazeeruddin, M. K.; Liska, P.; Péchy, P.; Grätzel, M. *Prog. Photovolt: Res. Appl.* **2007**, *15*, 603. (b) Ito, S.; Murakami, T. N.; Comte, P.; Liska, P.; Grätzel, C.; Nazeeruddin, M. K.; Grätzel, M. *Thin Solid Films* **2008**, *516*, 4613.
12. Gao, F.; Wang, Y.; Shi, D.; Zhang, J.; Wang, M.; Jing, X.; Humphry-Baker, R.; Wang, P.; Zakeeruddin, S. M.; Grätzel, M. *J. Am. Chem. Soc.* **2008**, *130*, 10720.
13. Chen, C.-C.; Chung, H.-W.; Chen, C.-H.; Lu, H.-P.; Lan, C.-M.; Chen, S.-F.; Luo, L.-Y.; Hung, C.-S.; Diau, E. W.-G. *J. Phys. Chem. C* **2008**, *112*, 19151.
14. Shi, D.; Pootrakulchote, N.; Li, R.; Guo, J.; Wang, Y.; Zakeeruddin, S. M.; Gratzel, M.; Wang, P. *J. Phys. Chem. C* **2008**, *112*, 17046.